

Akram Alhussein ^{1,2}, Julien Capelle ¹, Joseph Gilgert ¹, Saïd Hariri ³, Zitouni Azari ¹

DAMAGE OF PIPELINES BY SANDBLASTING AND HYDROGEN OŠTEĆENJA CEVOVODA PESKIRANJEM I VODONIKOM

Original scientific paper
UDC: 620.169.1 : 621.643.2
Paper received: 31.01.2011

Author's address:

¹) Laboratoire de Mécanique, Biomécanique, Polymères, Structures (LaBPS), Ecole Nationale d'Ingénieurs de Metz – Université Paul Verlaine de Metz, Metz, France

²) Laboratoire Universitaire des Sciences Appliquées de Cherbourg (LUSAC), ESIX Prod. Normandie, Cherbourg-Octeville, France

³) Département Technologie de, Polymères et Composites et Ingénierie Mécanique, Ecole des Mines de Douai, Douai Cedex, France

Keywords

- pipeline
- sandblasting erosion
- electrolytic hydrogen
- mechanical properties
- residual stress analysis

Abstract

The mechanical behaviour evaluation of a pipeline notched under the impact of sand and hydrogen has been performed. Material damage is made by electrolytic hydrogen and by projecting corundum particles (aluminium oxide). The sandblasting and the hydrogen have little effect on the yield stress and ultimate strength. The pipe lifetime and elongation at fracture is clearly affected by hydrogen, which penetrates into the surface layers of the material and changes the local fracture mechanism. Despite the erosion of these layers under the sand impacting, their is mechanical property improvement: elongation at fracture and fatigue lifetime are shown. In order to justify these evolutions, a microstructural study is carried out. The observation of damage mode and distribution of residual stress under the notch tip show that the material hardening, the notch radius and the compressive stress play an important role in stabilizing the mechanical properties of the material.

INTRODUCTION

Erosion is a mechanical process that causes an eroded volume on the surface of a material. The erosion phenomenon of pipelines by sandblasting in petroleum industry is a problem which affects many industrial sectors. The shocks between the sand particles and the structure surface cause severe damage. It is manifested by spalling craters of different shapes and depths, /1/. The wall thickness is gradually reduced and the rupture occurs when the stresses in the crater reach a limiting threshold.

Ključne reči

- cevovod
- erozija peskiranjem
- elektrolitički vodonik
- mehaničke osobine
- analiza zaostalog napona

Izvod

Data je ocena mehaničkog ponašanja cevovoda sa zarezom pod dejstvom udara peskom i vodonikom. Oštećenje materijala je izvedeno elektrolitičkim vodonikom i usmeravanjem čestica korunda (aluminijum oksida). Peskiranje i vodonik imaju malog uticaja na napon tečenja i zateznu čvrstoću. Vek cevovoda i izduženje pri lomu je jasno uslovljeno vodonikom, koji prodire u površinske slojeve materijala i menja lokalni mehanizam loma. Uprkos eroziji ovih slojeva pod udarima peska, ipak ima poboljšanja mehaničkih osobina: izduženje pri lomu i vek zamaranja su prikazani. Radi dokazivanja ovakvog razvoja, takođe je urađena i analiza mikrostrukture. Posmatranjem oblika oštećenja i raspodele zaostalog napona ispod vrha zareza pokazuju da ojačavanje materijala, radijus zaobljenja zareza i pritisni napon imaju važnu ulogu u stabilizaciji mehaničkih osobina materijala.

The erosion rate increases according to the sanding duration up to a constant value, /2/. The authors /2/ divide the phenomenon of the eroded volume into four consecutive stages: the initial stage, characterized by high volume loss rate at the beginning of the test, the incubation stage (some cracks are observed because of the accumulating plastic deformation), the acceleration stage, and the maximum rate stage, where the original surface is completely removed.

The main parameters of erosion are: the exposure time, the kinetic energy of particles /3/, and the impact angle /4/. The mechanical, chemical and thermal actions are the cause of the material separation, but the means to achieve these actions, are different. According to Meng /5/, there are four main mechanisms of erosion by impact of solid particles: cutting, fatigue, brittle fracture, and melting.

To study the material fatigue after the sandblasting operation, many tests are made. The sand erosion process improves resistance to fatigue under stresses, /6-7/. This improvement comes from the introduction of residual stresses in compression at the hardened surface layers. Many studies show the benefits of the process on material fatigue. Vo /8/ shows an improvement of endurance limit and material lifetime. This improvement is due to the surface state which improves by limiting the micro concentrations of stresses. This allows a larger cleavage time.

In addition to the sandblasting effect on the pipeline (with API 5L X52 steel) damage, the hydrogen influence on the mechanical behaviour of the material is studied. Hydrogen being the smallest atom identified can move easily in the crystalline sites of steel. The hydrogen diffuses in steel according to the traditional mechanisms of hetero-diffusion at infinite dilution, /9/.

According to Sofronis /10/, in the presence of hydrogen, the yield stress increases slightly with hydrogen concentration. He proposes a linear evolution of the yield stress with the hydrogen concentration. Delafosse and Magnin /11/ show (for a pipeline X52 steel) that the yield stress is slightly affected by the presence of electrolytic hydrogen. Only the failure strain is dramatically reduced by hydrogen action. They also conclude that the ultimate strength varies very little.

Hydrogen influence on material plasticity is expressed by one of the following hypotheses:

1. *Atomic cohesion forces.* Oriani /12/ assume a local decrease of atomic network cohesive forces, due to the

presence of hydrogen in the matrix or at grain boundaries /13/ (or any other metallurgic defect). A crack can propagate when the applied tensile stress is sufficient to counterbalance the cohesion force of the network, modified by the hydrogen presence. Qiao /14/ shows that the high concentration of hydrogen, located at the crack tip level in steel XC80, is sufficient to get a rupture by cleavage. It can be conceived that the hydrogen absorption allows ductile fracture behaviour to be a brittle one.

2. *Initiation and propagation of cracks.* Delafosse and Magnin /11/, Mao and Li /15/ show that the effect of crack creation cannot be only linked to the presence of hydrogen, particularly in networks with centred cubic faces (CCF). Nothing, until now, allows to identify the hydrogen responsibility percentage at crack initiation. As against, if the crack is already formed, its propagation will be amplified.

3. *Hydrogen trapping by dislocations.* Bastien and Azou /16/ are the first to suggest that “hydrogen – dislocations” interactions are involved in the mechanism of embrittlement by hydrogen. This mechanism, based on the fact that hydrogen as a proton, could be transported by the dislocations and thus contributes to the creation of a micro-crack at a level of dislocation stacking.

EXPERIMENTAL PROCEDURE

Material

Mechanical tests were realized on specimens with API 5L X52 steel taken from a pipe in both directions, Figure 1: Longitudinal direction (L) and Transverse direction (T). This pipe has an external diameter of 610 mm and a thickness of 11 mm. This section is selected from the pipeline used in the European natural gas transporting network. The pipe is manufactured according to the standards of the American Petroleum Institute: API 5L X52. A measure of chemical characteristics is done on this material, Table 1.

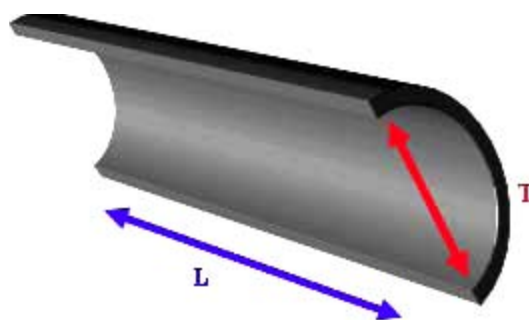


Figure 1. L and T directions of pipeline. Slika 1. Podužni (L) i poprečni (T) pravci cevovoda

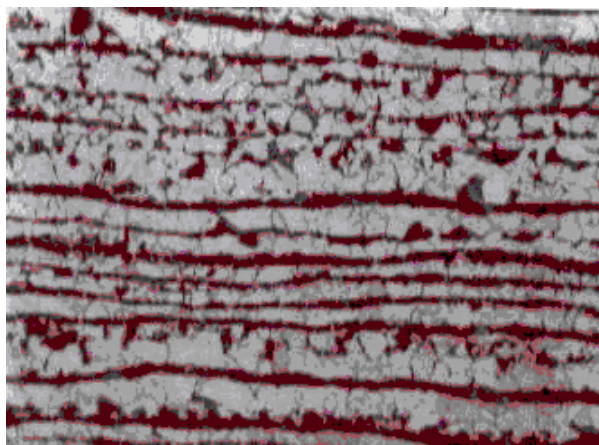


Figure 2. Microstructure of pipeline API 5L X52 steel. Slika 2. Mikrostruktura čelika cevovoda API 5L X52

Table 1. Chemical composition of pipeline API 5L X52 steel (wt %).

Tabela 1. Hemijski sastav čelika za cevovode API 5L X52 (tež. %)

C	Mn	Si	Cr	Ni	Mo	S	Cu	Ti	Nb	Al
0.206	1.257	0.293	0.014	0.017	0.006	0.009	0.011	0.001	< 0.03	0.034

The microstructure of pipeline API 5L X52 steel is analysed by optical microscopy after mechanical polishing and chemical treatment with Nital, Fig. 2. Metallographic analysis confirms that the sheet used in the manufacture of this pipe is rolled in both directions (L and T). The rolling rate in both directions may be different. Indeed, we observe bands of pearlite coloured in black alternating with bands of ferrite in white, which is a sign of rolling. We can also say that the ferrite is the main component of this structure. The microstructural study shows that the grain diameter ranges from 7 to 15 μm .

Sand erosion conditions

The basis of this study is to assess the pipeline damage by sand impacting. For this purpose, we used a Blaster 2700 sandblasting machine, equipped with a pressure

gauge, enabling it to adjust the desired power, Fig. 3. Sand supply (Al_2O_3) is ensured by the venturi effect, with a constant sand feed throughout the sandblasting operation. The air flow velocity (32 m/s) is measured by means of a wind gauge using an anemometer. It represents the average wind velocity or the sandblasting velocity in nature (especially in desert regions). It is evident that the flux velocity obtained by the anemometer does not correspond to the sand particles velocity. The sand particles velocity is not determined because of the complexity related to the variations in the nature, size and shape of sand. The sand grains have an angular shape and their average size is between 300 and 400 μm . Mechanical properties of the sand are presented in Table 2.

Table 2. Mechanical properties of sand (corundum) in air.

Tabela 2. Mehaničke osobine peska (korunda) na vazduhu

Hardness Vickers (HV)	Tensile strength (N/mm^2)	Bending strength (N/mm^2)	Compression strength (N/mm^2)	Young modulus (N/mm^2)	Poisson's ratio	Stress intensity factor ($\text{MPa}\cdot\text{m}^{1/2}$)
180–200	200–250	200–600	1900–2000	3.8×10^5	0.25–0.3	4–5

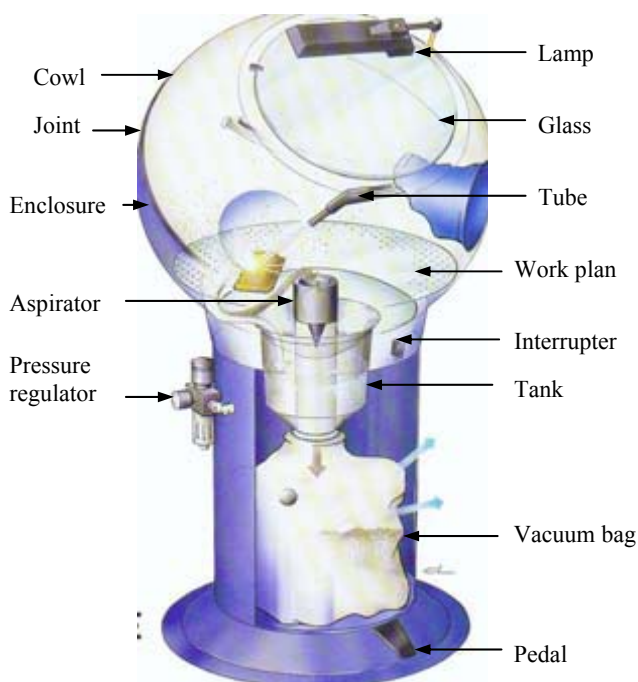


Figure 3. Blaster 2700 Sandblasting machine.

Slika 3. Blaster 2700 mašina za peskiranje

In order to adjust the projection angle of the abrasive and to concentrate the particle impact on a predefined area, an assembly is made, Fig. 4, with the following properties: nozzle diameter of 8 mm, an average sand feed during the erosion tests is about 1.57 g/s, an impact angle between the sand particles and the specimen surface is 90° , a distance between the nozzle and the specimen is 200 mm (allowing for sand particles to impact all of the notch area), an air pressure of 4 bar and a sandblasting duration varying between 60 and 480 min.



Figure 4. Specimen holder assembly.

Slika 4. Sklop držača epruvete

Damage conditions by hydrogen

Hydrogen in its gaseous state (H_2) is found in rare percentage on Earth. It is generally (99.98% of cases) recombined with other atoms in various materials (oil, water, metals, ...). To obtain hydrogen, different methods are used. In our study, hydrogen is produced by electrolysis of water (H_2O). At room temperature and up to 80°C , [17], electrolysis dissociates water molecules into two constituent atoms: oxygen and hydrogen, and introduces hydrogen at the electrode, which will be the loading specimen.

The charging cell, under electrolytic hydrogen, consists of two parts: a first box of homogenisation, where CO₂ and N₂ gas bubbles are made in order to stabilize the solution pH and to take off dissolved oxygen; a second box called “hydrogen-charging” contains the reference calomel electrode, the auxiliary electrode with platinum and working electrode corresponds to the specimen, Fig. 5.

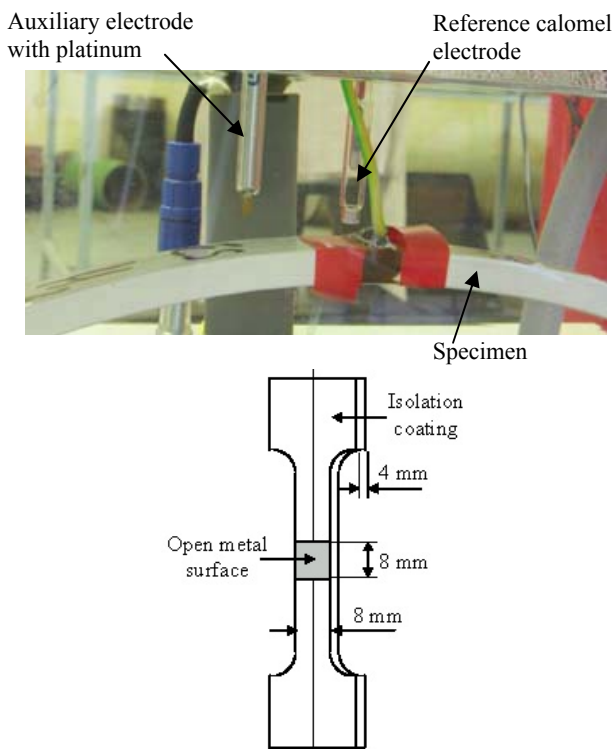


Figure 5. Specimen holder assembly.
Slika 5. Sklop držača epruvete

In order to perform the electrolysis process, it is necessary to have an external power source allowing an electron transfer reaction. A potentiostat will be used as a current source. It provides the capability to regulate the current to get the fixed potential.

The free potential (potential with the absence of external current) on the polarisation curve of pipeline API 5L X52 steel is -0.79 V_{sce}. This value complies with literature /18/ for this type of steel. To realize a reduction (cathode reaction), we apply a potential lower than this free potential value. Tests under electrolytic hydrogen will be realized at a constant potential of -1 V_{sce}, and in a standard electrolyte solution: NS4 (Natural Soil 4), for which the characteristics are given in Table 3.

Table 3. Chemical composition of NS4 solution (mg/litre).
Tabela 3. Hemijski sastav rastvora NS4 (mg/l)

KCl	NaHCO ₃	CaCl ₂ · 2H ₂ O	MgSO ₄ · 7H ₂ O
122	483	181	131

Electrolysis realization requires multiple electrodes, Fig. 5, /19/:

- Reference electrode is a saturated calomel electrode. It is used to control the applied tension.
- Auxiliary electrode is made of stainless steel (platinum), used to measure the evolution of current during the test.

- Working electrode is the specimen (hydrogen atoms are adsorbed on the surface of the specimen and with time they can diffuse towards interior of the specimen).

The solution pH is automatically controlled between 6.6 and 6.8. To keep this value during all the tests, we introduce discontinuous CO₂ gas bubbles by means of an optional rate valve.

During electrolysis, the aqueous solution produces oxygen. In order to deaerate the electrolytic solution, continuous nitrogen bubbles (N₂) are provided.

For electrolytic hydrogen charging and any type of the test realized, we use the parameters defined above. Figure 5 presents electrolysis electrodes with two different specimens.

RESULTS AND DISCUSSIONS

Static characteristics

The behaviour law of the material is obtained by performing tensile tests on specimens taken from a pipeline in both longitudinal and transverse (L and T) directions. The extraction and manufacturing of specimens are carried out so that the area (of the neutral plane) of a pipe coincides with that of tensile specimens. The specimen geometry is presented in Fig. 6.

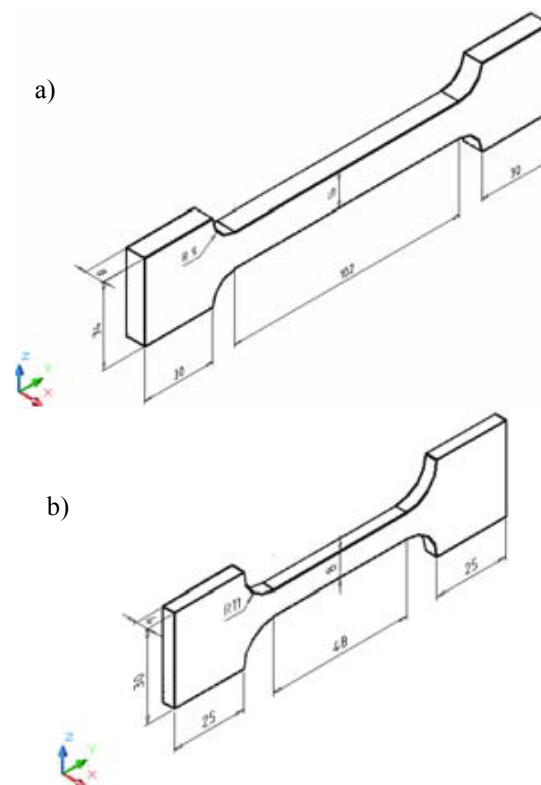


Figure 6. Tensile specimen geometry: a) L direction, b) T direction.

Slika 6. Geometrija zatezne epruvete: a) L pravac, b) T pravac

- a) In the longitudinal direction (L): tensile tests are realized on four specimens (L) of identical geometry: two original specimens treated as a reference, the other two impacted by sandblasting for eight hours; sanding is applied to one of the two specimen’s faces.
- b) In the transverse direction (T): tests are performed on eight specimens (T) of identical geometry: three refer-

ence specimens, three sanded for eight hours (sanding is applied to one of the two surfaces of the specimen) and two specimens charged with electrolytic hydrogen for one hundred hours. Only the useful zone, determined in the middle of the specimen (8 mm × 8 mm) is charged with hydrogen, Fig. 5. All other specimen surfaces are covered with anticorrosion paint, based on epoxy.

These tests are performed on the INSTRON 5585H machine, equipped with a static load cell of ±250 kN and pneumatic jaws, which is in agreement with the European standard /20/. The specimen tensile strain in both directions, longitudinal and transverse, is controlled by using a bidirectional video extensometer.

Table 4. Influence of sandblasting and hydrogen on the tensile properties of pipeline API 5L X52 steel in both directions: longitudinal (L) and transverse (T).

Tabela 4. Uticaj peskiranja i vodonika na zatezne osobine čelika cevovoda API 5L X52 u oba pravca: podužnom (L) i poprečnom (T)

Specimen type	Yield stress, σ_y (MPa)		Ultimate strength, σ_u (MPa)		Elongation at fracture, A (%)	
	L	T	L	T	L	T
Reference	318	450	548	626	24.94	18.17
Impacted by sand	322	429	561	574	34	21.23
Charged by hydrogen	–	420	–	570	–	10.56

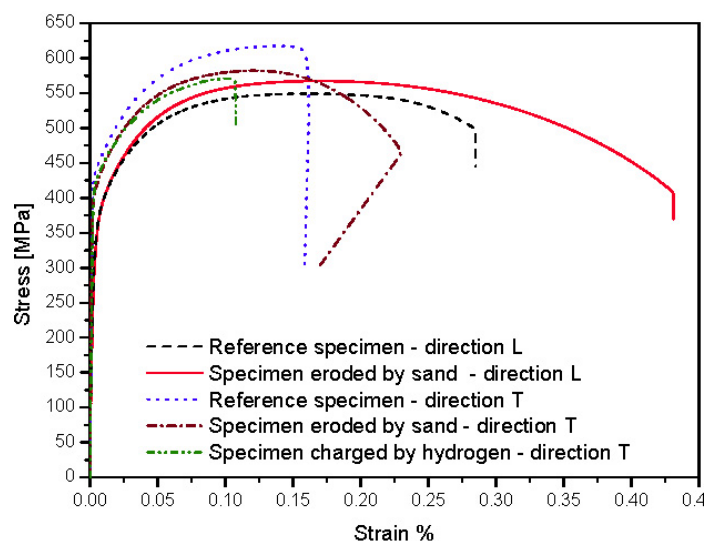


Figure 7. Behaviour law of pipeline API 5L X52 steel in both L and T directions.

Slika 7. Zakon ponašanja čelika cevovoda API 5L X52 za oba pravca L i T

The stress strain curves, Fig. 7, represent one test of each configuration. The average values of all tests are presented in Table 4.

In view of these results, it is possible to conclude that:

- Pipeline API X52 steel without pre-mechanical loading (reference specimens) is more resistant in the T than in the L direction. This behaviour is due to the ferrite and pearlite bands, which are more compressed in the T direction. This effect is produced during manufacturing of the pipe (rolling and welding).
- Material behaviour in both L and T directions, after eight hours of sanding, is different:
 - (a) In the L direction, the sandblasting increases all static mechanical characteristics. The increase of yield stress and ultimate strength is slight but the elongation at fracture is very large. It is about 36% more compared to reference specimens.
 - (b) In the T direction, sanding reduces yield stress by 4.7% and ultimate strength by 8.3% while the fracture strain is increased by 16.8%.
 - (c) In both L and T configurations, the sandblasting influence on static properties of the material is expressed by the increase of elongation at rupture. This advantage is

due to the plastification of surface layers impacted by sand, which increases material ductility.

- (d) In the presence of hydrogen, all tensile properties are lowered. Yield stress and ultimate strength are decreased by a small quantity, about 6.7% to 8.9% respectively. On the other side, elongation at fracture is considerably reduced as it can be seen in Table 4. Its obvious reduction (42%) is due to hydrogen absorption. Its presence, inside steel, modifies the stress strain behaviour of the material. Material fracture behaviour changes from ductile to brittle.

Fatigue characteristics

The purpose of these tests is to show the simultaneous influence of sandblasting and hydrogen on the material lifetime. In order to do that, several fatigue tests (3 point bending tests) on roman tile specimens are performed. Figure 8 shows the geometry of these specimens.

The fatigue lifetime evolution study of the material, notched, is carried out in two stages: *Specimen preparation* – these specimens are sandblasted during 8 hours. The geometry of the notch profile before and after sandblasting is measured, Fig. 9. The form and parameters of the notch are completely changed; *Realization of fatigue tests with or*

without hydrogen. Roman tile specimens used in fatigue tests are subjected to a sinusoidal loading and a load ratio of 0.5. The daily evolution of the internal pressure of these pipelines is between 40 and 70 bar. The average load

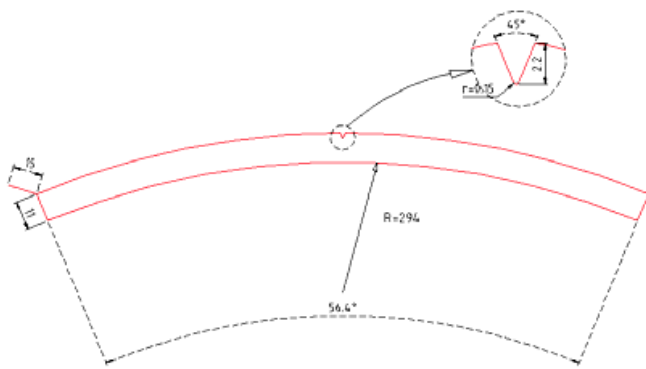


Figure 8. Fatigue specimen geometry: “Roman tile” specimen.
Slika 8. Geometrija epruvete za zamiranje: epruveta tipa „rimska ploča“

applied is between 750 and 2625 N. This load is applied on the opposite surface of the notch and in the middle of the horizontal distance between the two supports of 180 mm. The specimen section is 8.8 mm × 15 mm, Fig. 8.

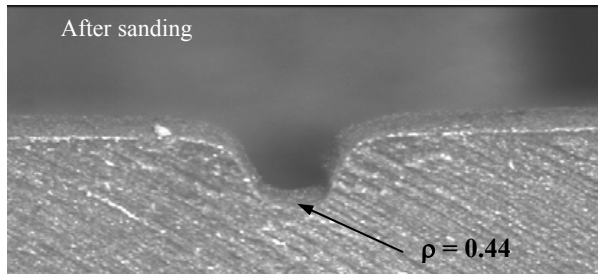
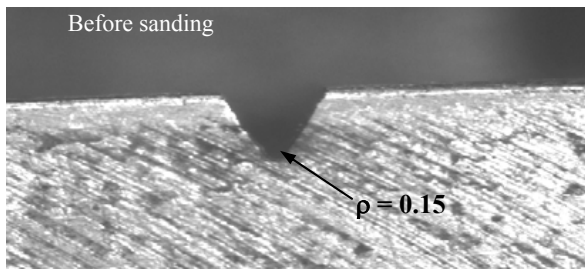


Figure 9. Notch profile geometry before and after 8 hours of sandblasting.
Slika 9. Profil geometrije zarez pre i nakon 8 sati peskiranja

The cycle frequency is between 1.7 and 10 Hz for tests in air, and kept constant at 0.05 Hz for tests in hydrogen. In the air, it is possible to change the frequency from one test to another, which is not the case in other environments, especially in the corrosion test [21]. The hydrogen effect, like all corrosion phenomena, needs time to penetrate and affect the steel [22]. It must be assured that the rupture is not entirely due to mechanical solicitations of the specimen.

For fatigue tests in hydrogen, a cell with Plexiglas, Fig. 10, is added in relation to the reference configuration in air. The primary function of this cell is to immerse the specimen

in the electrolytic solution (NS4) during the test. Electrolytic solution homogeneity is provided by a pump that sucked the solution at point A and pumped it back to point B.

Wöhler curves obtained from 3 point bending tests, for different cases, are presented in Fig. 11. These curves show that sandblasting increases life duration and hydrogen decreases it. The beneficial effect of sandblasting is due to three main parameters: a) local hardening; b) residual stresses are in compression at the notch bottom (Fig. 12); c) notch radius increases during sanding. After 8 hours of sanding, the radius increased from 0.15 to 0.44 mm, Fig. 9.

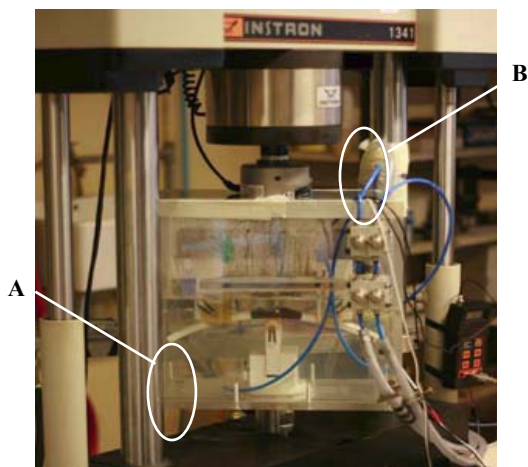


Figure 10. Assembly of 3 points bending test under hydrogen.
Slika 10. Sklop ispitivanja savijanjem u 3 tačke sa vodikom

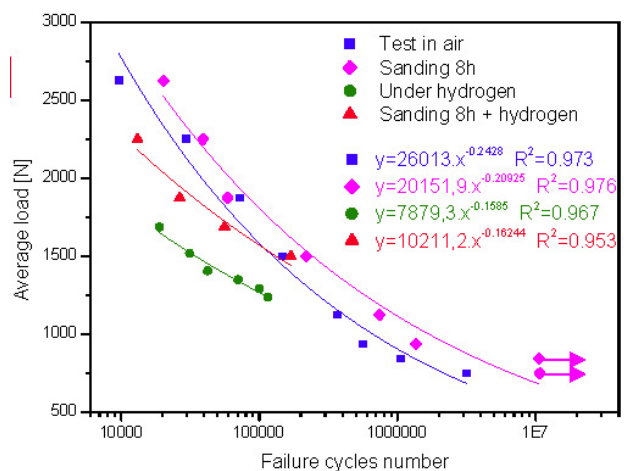


Figure 11. Wöhler curves for pipeline API 5L X52 steel.
Slika 11. Velerove krive za čelik cevovoda API 5L X52

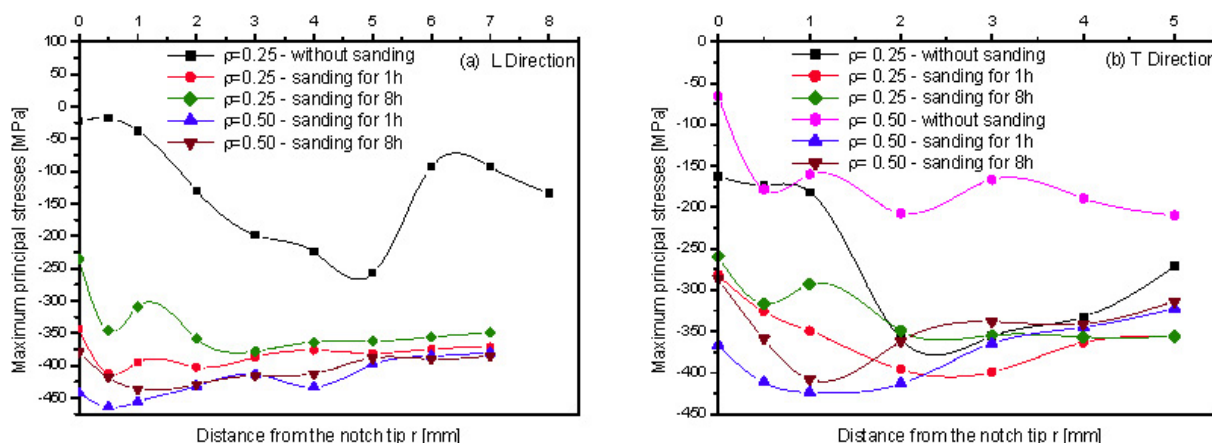


Figure 12. Variation of the maximum principal residual stresses at the notch bottom, for different values of notch radius and sanding time, in two directions: a) L direction, b) T direction.

Slika 12. Varijacija maksimalnih glavnih zaostalnih napona u dnu zarez, za različite vrednosti radijusa zarez i vremena peskiranja, za dva pravca: a) L pravac, b) T pravac

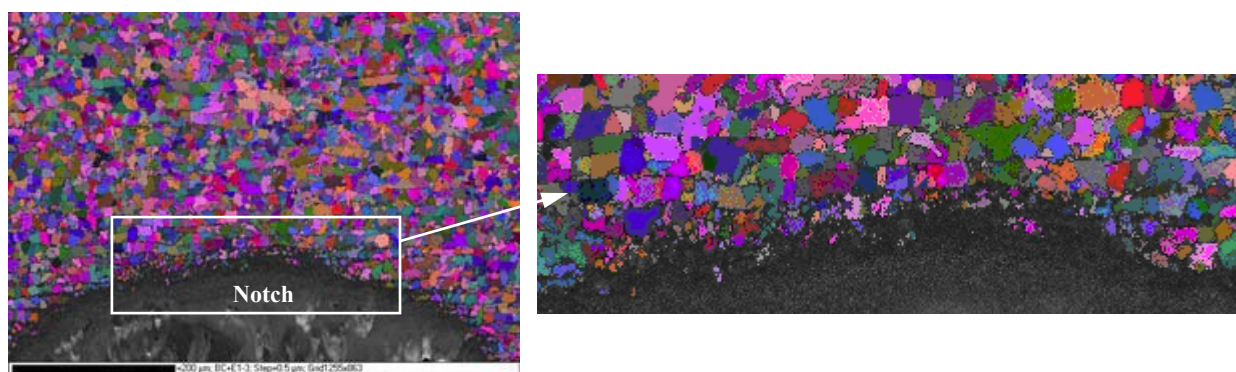


Figure 13. Microstructure of API 5L X52 steel eroded during 8h.
Slika 13. Mikrostruktura čelika API 5L X52 posle 8 sati erozije

The gain in material lifetime by sandblasting, compared with the reference one (fatigue test in air carried out on reference specimens), is a function of applied load. This value varies from 32% at the highest load (more than 2250 N) to 143% for a load less than 1000 N.

By comparing the lifetime curve under hydrogen with the other one in air, we notice that hydrogen is very harmful to the material life. It causes reduction to 81% for a load of 1688 N and 58% for a load of 1238 N. During three point bending test in hydrogen, the large density of dislocations in the middle of the specimen, where stresses are highest, act as traps for hydrogen. The hydrogen influence and material microstructural change (in terms of grain size, Fig. 13) are responsible for the severe drop in material lifetime.

Concerning the material affected by hydrogen and sand impact, lifetime depends on the applied load. For a high load, lifetime decreases (Fig. 11); it is -55% for a load of 2250 N. The more the applied loading decreases, the less important is the drop in lifetime. From a load of 1500 N, life duration is equivalent to that obtained for a specimen tested in air. The combined effect of hydrogen and sandblasting is then cancelled.

Residual stress analysis

This analysis allows us to answer the questions related to the evolution of mechanical properties of pipeline API 5L X52 steel under sandblasting. Residual stresses are measured

by X-ray diffraction, [23]. This measurement is performed on specimens with two values of notch radii: 0.25 and 0.50 mm. After conducting sandblasting tests for different time intervals, the measurements are taken at several points from notch tip and through specimen thickness (r). The plastification zone is just around the notch tip, so it is better to take the points very near to the notch.

The distribution of maximum principal residual stresses at the notch bottom in both L and T directions is presented in Fig. 12.

From these results, we find that:

- In all cases residual stresses are compressive. Sandblasting influences the level and distribution of residual stresses.
- The larger the notch radius, wider the impact area and higher are the residual stresses.
- After 1 hour of sandblasting, compressive stresses are more important than that after 8h of sandblasting. This situation is due to material hardening. At the beginning of erosion, the material hardens up to 1 hour of sandblasting. After this value, plastification starts, thus stress relaxation is followed by a more significant damage.
- In the L direction, we show that the sanding time until 1h produces more damage. We see a little difference between the two times (1 hour and 8 hours) starting from $r = 2$ mm for $\rho = 0.5$ mm and $r = 3$ mm for $\rho = 0.25$ mm.

- In the T direction, the same remarks as above are observed except that the stabilisation of residual stresses starts from $r = 4$ mm for both values of the notch radius.
- Compressive residual stresses introduced by sandblasting are more important in the L direction than in the T direction.

Variation of mechanical properties of pipeline API 5L X52 steel after sandblasting is due to material damage and microstructural evolution. In order to observe these changes, a scanning electron microscope (SEM) is used. Figure 13 illustrates the decrease of grain size at the notch tip. For a depth up to 10 μm , we can see the fragmentation of grains at the notch tip. This transformation is a sign of large plastic deformation.

CONCLUSIONS

Damage of pipelines notched with API 5L X52 steel, under sand impacting and with or without hydrogen, is studied. In order to evaluate material mechanical behaviour under sand erosion and hydrogen effect, tensile and fatigue tests are realized.

One of the first effects of sandblasting and hydrogen on API X52 steel is the significant variation of elongation at rupture. In the T direction, it is reduced by 42% in hydrogen and increased 16.8% after sandblasting. Yield stress and ultimate strength are slightly affected. Generally, these remarks can be considerable whatever the configurations direction of pipeline: longitudinal or transverse.

For fatigue, sand erosion improves the life duration of the pipeline, but hydrogen reduces it (it was reduced 73% for a load of 1400 N). Material lifetime under the influence of sand erosion and hydrogen depends on the applied load. The higher the load, the more important is the drop in lifetime. For low loads, it is remarkable that the fatigue curve of pipeline API 5L X52 steel sandblasted and charged with hydrogen, is relatively similar to that obtained in air. This is justified by the little deformations equivalent to that in the air.

Residual stress analysis at the notch bottom shows that at the beginning of erosion, the material undergoes hardening until one hour of sanding. After this value, plastification starts, thus stress relaxation is followed by more important damage. Material hardening, the notch radius and compressive residual stresses, play an important role on mechanical properties of the material. The hardening and damage are important parameters for estimating life duration of a structure, namely pipes.

REFERENCES

1. Hasan, F., Iqbal, J., *Consequential rupture of gas pipeline*, Eng Fail. Analysis, 2006, pp.127-135.
2. Hattori, S., Nakao, E., *Cavitation erosion mechanisms and quantitative evaluation based on erosion particles*, Wear, 2002, pp.839-845.
3. Wood, R.J.K., Puget, Y., Trethewey, K.R., Stokes, K., *The performance of marine coatings and pipe materials under fluid-borne sand erosion*, Wear, 1998, pp.46-59.
4. Bozzini, B., Ricotti, M.E., Boniadri, M., Mele, C., *Evaluation of erosion - corrosion in multiphase flow via CFD and experimental analysis*, Wear, 2003, pp.237-245.
5. Meng, H.C., Ludema, K.C., *Wear models and predictive equations: their form and content*, Wear, 1995, pp.443-457.
6. Lillamand, I., *Evolution d'une couche grenailée sous sollicitations thermiques et mécaniques: cas de la fatigue oligocyclique*, Thèse ENSAM, 1998.
7. Kirk, D., Render, P.E., *Effects of peening on stress corrosion cracking in carbon steel*, Proceed. of ICSP7, 1999, Warsaw-Poland.
8. Vo, L.D., Stephens, R.I., *Effect of Shot and Laser Peening on SAE 1010 Steel Tubes with a Transverse Center Weld Subjected to Constant and Variable Amplitude Loading*, Proceed. of 12th ICF, 2009, Canada.
9. Dayal, R-K., Parvathavarthini, N., *Hydrogen embrittlement in power plant steels*, Sadhana, 2003, Vol. 28.
10. Sofronis, P., Liang, Y., Aravas, N., *Hydrogen induced shear localisation of the plastic flow in metals and alloys*, Eur J of Mech -A/Solids, 2001, pp.857-872.
11. Delafosse, D., Magnin, T., *Hydrogen induced plasticity in stress corrosion cracking of engineering systems*, Eng Fract Mech, 2001, pp.693-729.
12. Oriani, R.A., Corrosion, 1987, Vol. 43, N°7, p.390.
13. Delafosse, D., Bayle, B., Bosch, C., *The roles of crack-tip plasticity, anodic dissolution and hydrogen in SCC of mild and C-Mn steels*, Envir-Induced Cracking of Materials, 2008, pp.267-278.
14. Qiao, L.J., Luo, J.L., Mao, X., Corrosion, 1998, Vol.54, N°2, p.115-120.
15. Scoot, X. Mao, Li, M., *Mechanics and thermodynamics on the stress and hydrogen interaction in crack tip stress corrosion: experiment and theory*, J Mech Phys Solids, 1998, pp.1125.
16. Bastien, P., Azou, P., *Influence de l'écrouissage sur le frottement intérieur de fer et de l'acier: chargé ou non en hydrogène*, C. R. Ac. Sc. 232, 1951, Paris, pp.1845.
17. Brass, A., Chene, J., Coudreuse, L., *Fragilisation des aciers par l'hydrogène: étude et prévention*, Les Techniques de l'Ingénieurs, M175, 2000.
18. Morales-Gil, P., Negrón-Silva, G., Romero-Romo, M., Ángeles-Chávez, C., Palomar-Pardavé, M., *Corrosion inhibition of pipeline steel grade API 5L X52 immersed in a 1 m H₂SO₄ aqueous solution using heterocyclic organic molecules*, Electrochimica Acta, 2004, pp.4733-4741.
19. Capelle, J., Gilgert, J., Dmytrakh, I., Pluvillage, G., *Sensitivity of pipelines with steel API X52 to hydrogen embrittlement*, Int J of Hydrogen Energy, 2008, pp.7630-7641.
20. NF A 03-001, NF EN 10002-1, Essai de traction, Partie 1: Méthode d'essai, AFNOR, 1990.
21. Zhongping, Y., Zhaohua, J., Xuetong, S., Shigang, X., Zhendong, W., *Influence of the frequency on the structure and corrosion resistance of ceramic coatings on Ti-6Al-4V alloy produced by microplasma oxidation*, Mats Chem and Phys, 2005, pp.408-412.
22. International Standard ISO 7539-9, Corrosion of metals and alloys – Stress corrosion testing, Part 9: Preparation and use of pre-cracked specimens for tests under rising load or rising displacement, 2003.
23. NF XP A 09-285, Essais non destructifs-Méthode d'essai pour l'analyse des contraintes résiduelles par diffraction des rayons X, AFNOR, 1999.